ELSEVIER

Journal of Molecular Structure: THEOCHEM 778 (2006) 49–53

THEO CHEM

www.elsevier.com/locate/theochem

Computational study of hydrogen bonding interaction between formamide and nitrosyl hydride

Ying Liu [a,c,*], Wenqing Liu [a], Haiyang Li [a,b], Yong Yang [a,c], Shuang Cheng [a,c]

[a] *Key Laboratory of Environmental Optical and Technology, Anhui Institute of Optics and Fine Mechanics, Chinese Academy of Sciences, Hefei 230031, PR China*

[b] *Dalian Institute of Chemical Physics, Chinese Academy of Sciences, Dalian 116023, PR China*

[c] *Graduate School of Chinese Academy of Sciences, Beijing 100039, PR China*

Received 9 December 2005; received in revised form 14 July 2006; accepted 31 July 2006
Available online 10 August 2006

Abstract

The hydrogen bonding interaction of formamide–nitrosyl hydride complex has been investigated using density functional theory (DFT) and ab initio method. The natural bond orbital (NBO) analysis and atom in molecules (AIM) theory were applied to understand the nature of the interaction. Two stable geometries are found on the potential energy surface, a six-membered cyclic structure of complex A and a seven-membered cyclic structure of complex B, characterized by AIM analysis. Complex A is less stable than complex B. It is confirmed that there are contractions of C—H (compared with the monomer $HCONH_2$), N—H bonds (compared with the monomer HNO) and the corresponding stretching vibrational frequencies are blue-shifted, while there is an elongation of the N—H bond and the corresponding stretching vibrational frequency is red-shifted, relative to those of the monomer $HCONH_2$. From NBO analysis, it is evident that the electron densities in the σ^* (C—H) and σ^*(N—H) of the complex A are less than those of the monomers $HCONH_2$ and HNO, which strengthen C—H and N—H bonds. Furthermore, the increases in s-characters of X also strengthen X—H bonds.

Keywords: Density functional theory (DFT); Hyperconjugation; Rehybridization; Electron density redistribution

1. Introduction

The amide functional group is important because the amide peptide bond is the basic linkage in peptides and proteins. The geometric constraints of the amide bond, such as the nearly planar structure around the C—N bond caused by its partial double bond character, define the conformational freedom of motion for many small molecules as well as for peptides and proteins. The study of van der Waals and hydrogen bonding interaction is significant to understand the structures of biological macromolecules, such as proteins and polynucleic acids. Formamide is the simplest molecule that contains a peptide linkage built by the carbonyl and amino groups. In the recent years, the hydrogen bonding interactions of formamide with small molecules have attracted much attention [1–8]. Zhou et al. investigated formamide–water and formamide–formamide dimers in the gas and solution using the density functional theory employing different basis sets [9,10]. Recently, Bende et al. have investigated the basis set supposition error (BSSE)-corrected geometrical structures, interaction energies and vibrational frequencies of those dimers, which agree satisfactorily with the experimental data [11]. However, most of these studies were devoted to the hydrogen bonding interactions of formamide and some stable molecules. The number of studies on those of formamide and radicals is much limited [12]. The hydrogen bonding interactions of stable molecules and radical, or radical and radical systems have been paid much attention due to its importance in the atmospheric and biological chemistry in recent years [13–18]. To the best of our knowledge,

* Corresponding author. Tel./fax: +86 551 559 1550.
E-mail address: lying@aiofm.ac.cn (Y. Liu).

0166-1280/$ - see front matter © 2006 Elsevier B.V. All rights reserved.
doi:10.1016/j.theochem.2006.07.023

there are no experimental and theoretical reports on the hydrogen bond formation between $HCONH_2$ and HNO. It has motivated the theoretical prediction of the $HCONH_2\cdots HNO$ complex for the further experimental studies.

This work focuses on the hydrogen bonding interaction of $HCONH_2\cdots HNO$ complex. The optimized geometries, interaction energies and vibrational frequencies of this system were calculated by standard and counterpoise (CP) correction methods using density functional theory and ab initio method. AIM and NBO analyses were carried out to provide more information on the complex. It theoretically provided information on the hydrogen bonding interaction of $HCONH_2\cdots HNO$ complex and explained the blue- and red-shifts of N—H, C—H stretching vibrational frequencies.

2. Computational methods

Geometrical structures, vibrational frequencies and interaction energies of this system were determined at second-order Møller-Plesset perturbation (MP2) and Becke's three parameter hybrid functional in conjunction with Lee, Yang, and Parr's correlation functional (B3LYP) levels employing 6-311++G(3df,3pd) basis set. The effect of the CP method, which was performed at B3LYP/6-311++G (3df,3pd) level, to the BSSE in the calculations of geometrical optimizations, vibrational frequencies and interaction energies has been taken into account [19]. Such a procedure often gives more reliable results than those obtained by the standard procedure, comparing with the experimental data [11,20–24]. G3B3 method was also applied to estimate the interaction energies of the complexes.

Both AIM and NBO analyses were performed at B3LYP/6-311++G (3df,3pd) level. AIM theory of Bader was used to analyze the bonding characteristics, which is based on a topological analysis of ρ and $\nabla^2\rho$ [25]. According to the topological analysis of electron density in the theory of AIM, ρ is used to describe the strength of a bond. The $\nabla^2\rho$ describes the characteristic of the bond. Where $\nabla^2\rho < 0$, it is named as the covalent bond, as $\nabla^2\rho > 0$, it is referred to a closed-shell interaction and is characteristic of the ionic bond, hydrogen bond or van der Waals interaction. Here, $\nabla^2\rho = \lambda_1 + \lambda_2 + \lambda_3$, λ_i is an eigenvalue of the Hessian matrix of ρ. When one of the three λ_i is positive and the other two are negative, we denote it by $(3,-1)$ and call it the bond critical point (BCP). When one of the three λ_i is negative and the other two are positive, we denote it by $(3,+1)$ and call it the ring critical point (RCP), which indicates that a ring structure exists. There are a set of criteria for ρ and $\nabla^2\rho$ proposed at BCPs for the hydrogen bonds [26]. However, the criteria proposed are exceeded by those of the reported hydrogen bonding interactions [12,27]. Then, the analysis went further with parameters obtained by means of NBO theory of Weihnhold and co-workers at B3LYP/6-311++G (3df,3pd) level [28]. All calculations were carried out using the Gaussian03 package [29].

3. Results and discussion

3.1. Geometries, frequencies and energies

Geometrical characteristics of complexes A and B were summarized in Table 1. Table 2 listed bond length variations and vibrational frequency shifts in contrast to monomers. The optimized structures of the complexes were depicted in Fig. 1.

Complex A has a cyclic configuration. The r(H2···O9) and r(H7···O3) are 2.7898 and 2.0774 (B3LYP), 2.6508 and 2.0671 (MP2), 2.8152 and 2.0921 Å (B3LYP-CP-corrected). The CP-corrected r(H···X) are a little longer than the uncorrected ones. Complex B also has a cyclic configuration. The r(H7···O3) and r(H5···O9) are 2.0053 and 2.0804 (B3LYP), 2.0003 and 2.0532 (MP2), 2.0135 and 2.1028 Å (B3LYP-CP-corrected). All calculations show that r(H7···O3) in the complex B is shorter than that in the complex A. From Table 1, the interaction energies obtained is −3.42 (B3LYP), −3.19 (B3LYP-CP-corrected),

Table 1
Optimized bond lengths (Å), bond angles (°) and interaction energies (kcal/mol) of the complexes A and B with different standard optimizations at B3LYP, MP2 levels and CP-corrected optimization at B3LYP level in conjunction with 6-311++G(3df,3pd) basis set

		B3LYP	MP2	$B3LYP_{CP}$
Complex A	r(C1—H2)	1.1	1.0968	1.1002
	r(C1—O3)	1.2161	1.2202	1.2159
	r(C1—N4)	1.3506	1.3511	1.3506
	r(N4—H5)	1.0073	1.0058	1.0072
	r(N4—H6)	1.0045	1.003	1.0045
	r(N8—H7)	1.0535	1.0442	1.0537
	r(N8—O9)	1.2052	1.2246	1.2049
	r(H2···O9)	2.7898	2.6508	2.8152
	r(H7···O3)	2.0774	2.0671	2.0921
	∠H2C1N4	113.46	113.60	113.43
	∠H5N4C1	119.68	119.44	119.67
	∠O3C1N4	124.31	124.09	124.32
	∠H6N4C1	121.13	120.92	121.13
	∠H7N8O9	107.59	106.42	107.66
	ΔE	−3.42	−4.62	−3.19
Complex B	r(C1—H2)	1.1009	1.0974	1.1012
	r(C1—O3)	1.2192	1.2226	1.2189
	r(C1—N4)	1.3453	1.3464	1.3456
	r(N4—H5)	1.0153	1.0126	1.015
	r(N4—H6)	1.0045	1.0031	1.0046
	r(N8—H7)	1.0557	1.0464	1.0558
	r(N8—O9)	1.2075	1.2256	1.207
	r(H5···O9)	2.0804	2.0532	2.1028
	r(H7···O3)	2.0053	2.0003	2.0135
	∠H2C1N4	113.60	113.57	113.52
	∠O3C1N4	124.73	124.53	124.81
	∠H5N4C1	119.13	118.96	119.24
	∠H6N4C1	120.81	120.54	120.77
	∠H7N8O9	107.96	107.00	107.97
	ΔE	−5.27	−6.61	−4.90

Table 2
Bond length variations (Å) and vibrational frequency shifts (cm^{-1}) with respect to monomers by B3LYP, MP2 standard calculations and CP-corrected optimization at B3LYP methods employing 6-311++G(3df,3pd) basis set

		B3LYP	MP2	$B3LYP_{CP}$
Complex A	Δr(C1—H2)	−0.0044	−0.0033	−0.0042
	Δr(N8—H7)	−0.0082	−0.0058	−0.008
	$\Delta \nu$(C1—H2)	+53	+46	+51
	$\Delta \nu$(N8—H7)	+144	+117	+140
Complex B	Δr(N8—H7)	−0.006	−0.0036	−0.0059
	Δr(N4—H5)	+0.0082	+0.0072	+0.0079
	$\Delta \nu$(N8—H7)	+122	+88	+118
	$\Delta \nu_{symm.}$(N4—H5)	−115	−100	−110
	$\Delta \nu_{assymm.}$(N4—H5)	−33	−33	−33

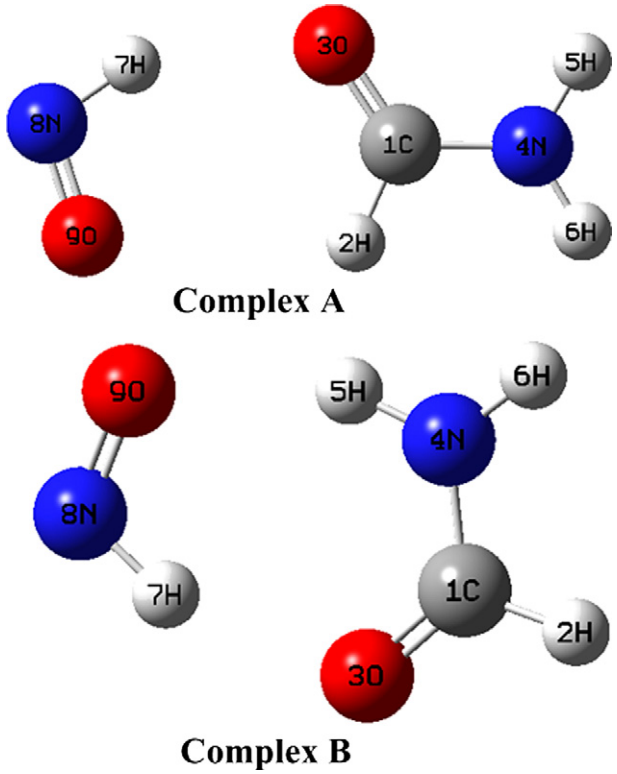

Fig. 1. The optimized $HCONH_2\cdots HNO$ complex at B3LYP/6-311++G (3df,3pd) level.

−3.79 (G3B3), −4.62 kcal/mol (MP2) for the complex A and −5.27 (B3LYP), −4.90 (B3LYP-CP-corrected), −5.97 (G3B3), −6.61 kcal/mol (MP2) for the complex B. All calculations indicate the complex B is more stable than the complex A. Complex B is the global minimum and complex A is the local minimum.

By examining Table 2, it becomes evident that there are contractions of N8—H7, C1—H2 bonds and an elongation of the N4—H5 bond. The shortened degrees for N8—H7, C1—H2 bonds obtained at MP2 level are smaller than those obtained at B3LYP level, while it is opposite to the elongated degree of the N4—H5 bond. The corresponding N8—H7 and C1—H2 stretching vibrational frequencies are blue-shifted while the N4—H5 stretching vibrational frequency is red-shifted relative to monomers. In contrast to the results obtained by CP-corrected calculations, the blue-shift degrees of N8—H7 and C1—H2 stretching vibrational frequencies obtained by standard calculations are a little larger. The red-shift degree of the N4—H5 stretching vibrational frequency is a little smaller. On the basis of these analyses, it can be confirmed that the complex A simultaneously possesses two blue-shifts of ν(N8—H7) and ν(C1—H2).The complex B simultaneously exhibits a red-shift of ν(N4—H5) and a blue-shift of ν(N8—H7).

3.2. AIM analysis

To characterize the interaction within the system considered in the present study, several basic parameters arising from Bader's theory of AIM were calculated. The corresponding results were listed in Table 3. As shown in Table 3, the values of ρ for O3···H7 and O2···H9 in the complex A are 0.021 and 0.006 a.u., which of $\nabla^2\rho$ are 0.069 and 0.020 a.u., respectively. The values of ρ for O3···H7 and O5···H9 in the complex B are 0.025 and 0.020 a.u., which of $\nabla^2\rho$ are 0.078 and 0.065 a.u., respectively. All $\nabla^2\rho$ at BCPs are positive, which indicate they are closed-shell interactions. From Table 1, the r(O3···H7) of the complex B is shorter than that of the complex A. The corresponding ρ(O3···H7) of the complex B is more than that of the complex A. The increase in distance (O3···H7) results in reducing orbital overlap, therefore, the corresponding ρ(O3···H7) decreases. In addition, it is worthy of mentioning that there are RCPs in the complexes A and B, respectively, which indicate there are a six-membered ring C1—H2—O9—N8—H7—O3 in the complex A and a seven-membered ring C1—O3—H7—N8—O9—H4—N5 in the complex B.

3.3. NBO analysis

To get more information on the blue-shifts of C1—H2, N8—H7 vibrational frequencies and the red-shift of the N4—H5 vibrational frequency, NBO analysis was

Table 3
Topological parameters (a.u.) of the BCPs and RCPs at the B3LYP/6-311++G(3df,3pd) level

BCP	ρ	$\nabla^2\rho$	λ_1	λ_2	λ_3
Complex A					
O3···H7	0.021	0.069	−0.027	−0.026	0.122
O9···H2	0.006	0.020	−0.005	−0.004	0.028
RCP					
C1H2O9N8H7O3	0.005	0.024	−0.004	0.004	0.023
Complex B					
O3···H7	0.025	0.078	−0.034	−0.033	0.144
O5···H9	0.020	0.065	−0.027	−0.026	0.119
RCP					
C1O3H7N8O9H4N5	0.006	0.028	−0.005	0.014	0.019

performed at B3LYP/6-311++G (3df,3pd) level. The corresponding results were listed in Table 4.

The importance of hyperconjugation and electron density transfer (EDT) from lone electron pairs of the Y atom to the X—H antibonding orbital in the X—H···Y system is well documented [28]. In general, such interaction leads to an increase in population of X—H antibonding orbital. The increase of electron density in X—H antibonding orbital weakens the X—H bond, which leads to its elongation and constrains the blue shift of the X—H stretching frequency. Hobza proposed that electron density redistribution is related to the contraction of X—H bond [30,31]. Recently, it has been reported that the change of electron density in the σ^*(X—H), compared with the monomer, is a combination of two effects for the Z (or Z—W)—X—H···Y(or Y—U) H-bond [32]: the increase of the electron density in the σ^*(X—H) due to hyperconjugation (n(Y) or σ(Y—U) $\rightarrow \sigma^*$ (X—H)) while the decrease of the electron density in the σ^* (X—H) due to the electron density redistribution (n(Z) or σ(Z—W) $\rightarrow \sigma^*$(X—H)). From Table 4, the electron densities in both σ^*(C1—H2) and σ^*(N8—H7) of the complex A decrease, implying the electron density redistribution exceeds hyperconjugation, which strengthen C1—H2 and N8—H7 bonds and contribute to blue-shifts of stretching vibrational frequencies. For the complex B, it is evident the increases of the electron densities occur in the σ^*(N4—H5) and σ^*(N8—H7) and weaken N4—H5 and N8—H7 bonds, which contribute to the red-shifts of corresponding stretching vibrational frequencies.

The chemical perspective has been suggested to explain 'proper' and 'improper hydrogen bonding': the hyperconjugation (n(Y) $\rightarrow \sigma^*$(X—H)) can be balanced by the increase in s-character and polarization of the X—H bond [33]. The authors show that the X—H bond strengthening effect is an increase in s-character of X hybrid orbital in the X—H bond, which is a direct consequence of Bent's rule. According to this rule, atoms tend to maximize the amount of s-character in hybrid orbital with the larger amount of p-character toward more electronegative substituents. As a result, a decrease in effective electronegativity of hydrogen in an X—H bond leads to an increase in the s-character of the hybrid orbital and results in the corresponding bond polarization's increase. As listed in Table 4, the changes in the electronic structure of the complex A are an increase of positive charge on H2 atom and a simultaneous increase of negative charge on C1 atom, which lead to the increase in the C1—H2 bond polarization. It results in the increase in the s-character of the carbon hybrid orbital in C1—H2 bonds, which strengthens the C1—H2 bond. Similarly, the increases of positive charges on H7 atoms are accompanied by the simultaneous increases of the negative charges on N8 atoms of the complexes A and B. The N8—H7 bonds become more polarized. All lead to the increases in the s-characters of the nitrogen hybrid orbital in N8—H7 bonds, which strengthen the N8—H7 bonds. For the N4—H5 bond, the positive charge on H4 atom increases, compared to the monomer, while the negative charge on N5 atom decreases. These variations still result in the increase in the s-character of the nitrogen hybrid orbital in the N4—H5 bond, which contributes to the contraction of the N4—H5 bond.

To summarize, for the complexes, the changes of electron density in the σ^*(X—H) and s-character in the X hybrid orbital of X—H bond compared with the monomer are crucial to the elongation and contraction of the X—H bond. As to the complex A, the decreases of the electron densities in the σ^*(C1—H2) and σ^*(N8—H7) due to the electron density redistribution and the increases of s-characters in C1 and N8 atoms due to rehybridization strengthen the C1—H2 and N8—H7 bonds, which result in the blue-shifts of C1—H2 and N8—H7 stretching vibrational frequencies. For the complex B, the weakening effect owning to the increase of the electron density in the σ^*(N4—H5) exceeds the strengthening effect owning to the increase of s-character in N4 atom and thereby it leads to the elongation of the

Table 4
NBO analysis of the monomers and complexes at the B3LYP/6-311++G(3df,3pd) level

	HNO	$HCONH_2$	Complex A	Complex B
$\Delta\sigma^*$(C1—H2)/e			−0.00807	
$\Delta\sigma^*$(N8—H7)/e			−0.00344	+0.00149
$\Delta\sigma^*$(N4—H5)/e				+0.01801
q(C1)/e		0.54852	0.55191	
q(H2)/e		0.09265	0.11593	
spn(C1—H2)		$sp^{2.12}$	$sp^{2.07}$	
% s-char(C in C1—H2)		32.04	32.51	
q(N8)/e	0.00573		−0.02107	−0.00281
q(H7)/e	0.23878		0.29424	0.30422
spn(N8—H7)	$Sp^{4.58}$		$sp^{3.81}$	$sp^{3.65}$
% s-char(N in N8—H7)	17.97		20.75	21.45
q(N4)/e		−0.80680		−0.79871
q(H5)/e		0.39046		0.40722
spn(N4—H5)		$sp^{2.29}$		$sp^{2.15}$
% s-char(N in N4—H5)		30.37		31.66

N4—H5 bond, followed by a red-shift of the stretching vibrational frequency. On the contrary, the weakening effect owning to the increase of the electron density in the σ^*(N8—H7) is exceeded by the strengthening effect owning to the increase of s-character in N8 atom. As a result, it leads to the contraction of the N8—H7 bond and a blue-shift of corresponding stretching vibrational frequency.

Acknowledgements

This work was supported by the Director Research Grants (2003) of Hefei Institute of Physical Science and Anhui Institute of Optics and Fine Mechanics, Chinese Academy of Science, and Center for Computational Science, Hefei Institutes of Physical Sciences under Grant No. 0330405002.

References

[1] F.J. Lovas, R.D. Suenram, G.T. Fraser, C.W. Gillies, J. Zozom, J. Chem. Phys. 88 (1988) 722.
[2] J.F. Hinton, R.D. Harpool, J. Am. Chem. Soc. 99 (1977) 349.
[3] A. Engdahl, B. Nelander, P.-O. Astrand, J. Chem. Phys. 99 (1993) 4894.
[4] E.M. Cabaleiro_Lago, J.R. Otero, J. Chem. Phys. 117 (2002) 1621.
[5] J. Park, J.-H. Ha, R.M. Hochstrasser, J. Chem. Phys. 121 (2004) 7281.
[6] N.A. Besley, J.D. Hirst, J. Am. Chem. Soc. 121 (1999) 8559.
[7] J. Florián, B.G. Johnson, J. Phys. Chem. 99 (1995) 5899.
[8] T. Neuheuser, B.A. Hess, C. Reutel, E. Weber, J. Phys. Chem. 98 (1994) 6459.
[9] A.P. Fu, D.M. Du, Z.Y. Zhou, J. Mol. Struct.(Theochem) 623 (2003) 315.
[10] J.F. Lu, Z.Y. Zhou, Q.Y. Wu, G. Zhao, J. Mol. Struct. (Theochem) 724 (2005) 107.
[11] A. Bende, S. Suhai, Int. J. Quantum Chem. 103 (2005) 841.
[12] M. Solimannejad, G. Azimi, L. Pejov. Chem. Phys. Lett. 400 (2004) 185.
[13] X.J. Qi, L. Liu, Y. Fu, Q.X. Guo, Struct. Chem. 16 (2005) 347.
[14] M. Lucarini, V. Mugnaini, G.F. Pedulli, M. Guerra, J. Am. Chem. Soc. 125 (2003) 8318.
[15] X.M. Zhou, Z.Y. Zhou, H. Fu, Y. Shi, H.T. Zhang, J. Mol. Struct. (Theochem) 714 (2005) 7.
[16] Y.H. Qu, X.F. Bian, Z.Y. Zhou, H.W. Gao, Chem. Phys. Lett. 366 (2002) 260.
[17] Z. Zhou, Y. Qu, L. Guo, H. Gao, X. Cheng, J. Mol. Struct. (Theochem) 586 (2002) 149.
[18] Z. Zhou, Y. Qu, A. Fu, D. Du, Int. J. Quantum Chem. 89 (2002) 550.
[19] S.F. Boys, F. Bernardi, Mol. Phys. 19 (1970) 553.
[20] A. Bende, Á. Vibók, G.J. Halász, S. Suhai, Int. J. Quantum Chem. 84 (2001) 617.
[21] P. Hobza, Z. Havlas, Chem. Rev. 100 (2000) 4253.
[22] S. Suhai, J. Chem. Phys. 103 (1995) 7030.
[23] I. Mayer, Int. J. Quantum Chem. 70 (1998) 41.
[24] P. Hobza, Z. Havlas, Theor. Chem. Acc. 99 (1998) 372.
[25] R.F.W. Bader, Atoms in Molecules: A Quantum Theory, Oxford University Press, Oxford, 1990.
[26] P.L.A. Popelier, J. Phys. Chem. A 102 (1998) 1873.
[27] P. Kolandaivel, V. Nirmala, J. Mol. Struct. 694 (2004) 33.
[28] A.E. Reed, L.A. Curtiss, F. Weinhold, Chem. Rev. 88 (1988) 899.
[29] M.J. Frisch, G.W. Trucks, H.B. Schlegel, G.E. Scuseria, M.A. Robb, J.R. Cheeseman, J.A. Montgomery, Jr., T. Vreven, K.N. Kudin, J.C. Burant, J.M. Millam, S.S. Iyengar, J. Tomasi, V. Barone, B. Mennucci, M. Cossi, G. Scalmani, N. Rega, G.A. Petersson, H. Nakatsuji, M. Hada, M. Ehara, K. Toyota, R. Fukuda, J. Hasegawa, M. Ishida, T. Nakajima, Y. Honda, O. Kitao, H. Nakai, M. Klene, X. Li, J.E. Knox, H.P. Hratchian, J.B. Cross, C. Adamo, J. Jaramillo, R. Gomperts, R.E. Stratmann, O. Yazyev, A.J. Austin, R. Cammi, C. Pomelli, J.W. Ochterski, P.Y. Ayala, K. Morokuma, G.A. Voth, P. Salvador, J.J. Dannenberg, V.G. Zakrzewski, S. Dapprich, A.D. Daniels, M.C. Strain, O. Farkas, D.K. Malick, A.D. Rabuck, K. Raghavachari, J.B. Foresman, J.V. Ortiz, Q. Cui, A.G. Baboul, S. Clifford, J. Cioslowski, B.B. Stefanov, G. Liu, A. Liashenko, P. Piskorz, I. Komaromi, R.L. Martin, D.J. Fox, T. Keith, M.A. Al-Laham, C.Y. Peng, A. Nanayakkara, M. Challacombe, P.M.W. Gill, B. Johnson, W. Chen, M.W. Wong, C. Gonzalez, J.A. Pople, Gaussian 03, Revision B. 02, Gaussian, Inc., Pittsburgh PA, 2003.
[30] J. Chocholoušová, V. Špirko, P. Hobza, Phys. Chem. Chem. Phys. 6 (2004) 37.
[31] P. Hobza, V. Špirko, Phys. Chem. Chem. Phys. 5 (2003) 1290.
[32] Y. Yang, W.J. Zhang, X.M. Gao, Int. J. Quantum Chem. 106 (2006) 1199.
[33] I.V. Alabugin, M. Manoharan, S. Peabody, F. Weinhold, J. Am. Chem. Soc. 125 (2003) 5973.